

Testing of Photomultiplier Tubes To Be Used for the GlueX Forward Calorimeter

Kei Moriya*,
Kevin Bauer,
Scott Henderson,
Indiana University Department of Physics

January 15, 2013

Abstract

The photomultiplier tubes (PMTs) to be used for readout of the GlueX Forward Calorimeter have been tested for gain dependence on high voltage. The tests were conducted over a period of several months, beginning in May 2011, and the procedures and results of these tests are described. The purpose of this note is to describe the procedure of how the PMTs were tested, and what the selection criteria were for choosing which PMTs to use in the final GlueX setup.

1 Introduction

The Forward Calorimeter (FCAL) of the GlueX detector will be an essential instrument in reconstructing many of the multi-particle final states that are expected to be produced in the GlueX Experiment. In this document we outline the procedures we took to calibrate the $\sim 3,000$ photomultiplier tubes (PMTs) to be used for individual modules of the FCAL.

The measurements involved setting up a light-tight environment where the PMTs were placed, and counting the number of counts that were either in or out of coincidence with an LED pulser that was flashed. Fits to these counts have been made, and a detailed analysis of these results will be shown below. Also, an additional goal of these measurements was to check that all PMTs were working as expected, and to ensure that their behavior was well understood. These results will be put in a database and the high voltage values of each module will be adjusted according to these measurements for initial gain balancing.

Setting up of the PMT tests began in the spring of 2011, and most of the setup was completed during the summer. Towards the end of the summer, most of our manpower had to be used on the beamtest that took place in Hall B of Jefferson Lab to test the 5×5 array of FCAL modules. Production runs for the PMT test started in the late fall of 2011, and most of the data were taken between January and May of 2012. Figure 1 shows the cumulative number of good PMTs that were measured with time (the definition of “good” will be given later). In total, close to 3,200 PMTs were tested, of which ~ 3100 were deemed as acceptable for the actual experiment.

In Section 2, the hardware used for these measurements will be introduced, along with the timing of our measurements and the electronics logic involved. In Section 3, a detailed analysis of our measurements and analysis will be given. Section 4 will show the various systematic effects that can affect our measurements, Section 5 will show the criteria we chose for the final selection of PMTs to be used in the final GlueX setup, and we will conclude in Section 6.

*kmoriya@indiana.edu

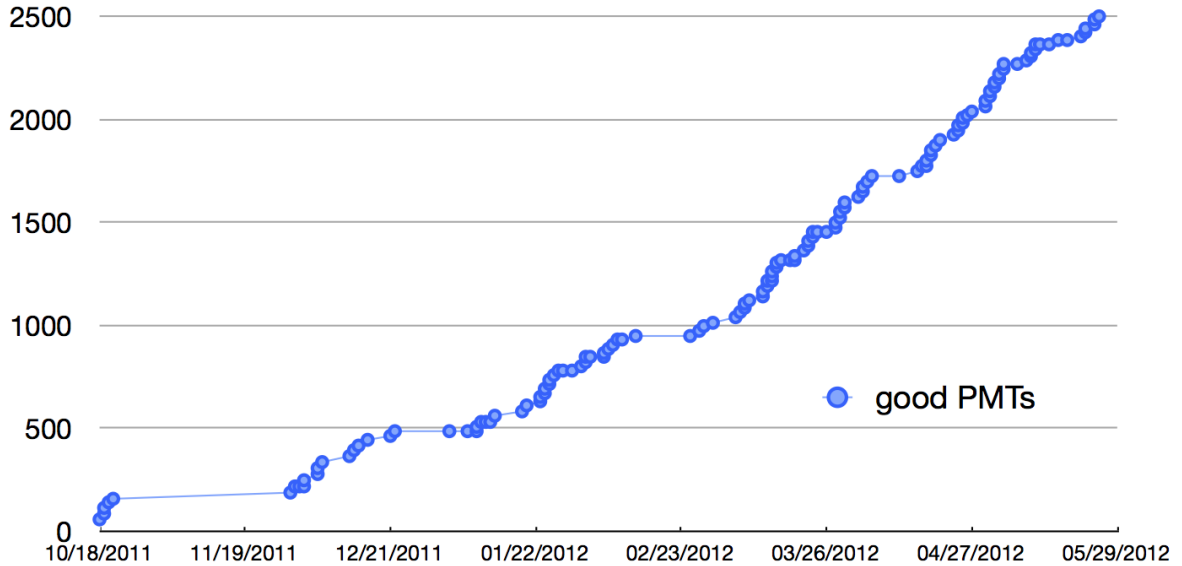


Figure 1: Cumulative counts of “good” PMTs over time. Production runs started in the fall of 2011, but had to be stopped for beamtest preparations. After the new year, production ramped up, with some breaks due to systematic issues. These counts do not include the retested PMTs.

2 Setup of Tests

The FCAL of the upcoming GlueX Experiment in Hall D of Jefferson Lab (JLab) will have 2,800 lead glass blocks, each individually coupled to a photomultiplier tube (PMT) and base for high voltage supply and remote control. Figure 2 shows an exploded view of each module.

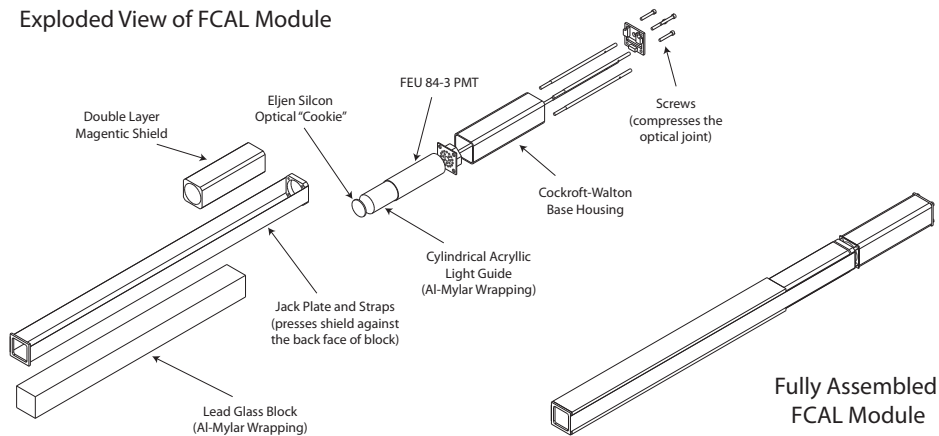


Figure 2: An exploded view of each component of the FCAL.

The focus of this paper is explaining the procedure of testing individual PMT that will be coupled to a single lead glass block for reading out the Čerenkov light produced by particles passing through them. The reason for doing these measurements are twofold. Since the characteristics of each PMT are different, knowledge of the size of the output signal at each high voltage setting is useful, and will be used to adjust the

initial high voltages on each module during the GlueX experiment. Also, since the PMTs are being reused from previous experiments, E852 at Brookhaven, and RadPhi at Hall B of Jefferson Lab, we want to ensure that the PMTs are still useful, and have not degraded largely since their last use.

Below in this section, we examine the hardware that was used, and the signal characteristics obtained from our measurements.

2.1 PMTs Used in the Tests

Figure 3 shows a picture of one of the PMTs used in our measurements. The PMTs are of type FEU84-3, which were used in the E852 Experiment at Brookhaven and the RadPhi Experiment at Hall B of Jefferson Lab. Recently, a new batch of ~ 440 PMTs of the same type have been acquired from Russia. All measurements have been done with the light guide glued on to the front of the PMTs, with a layer of very thin mylar surrounding the PMT for electrical insulation.

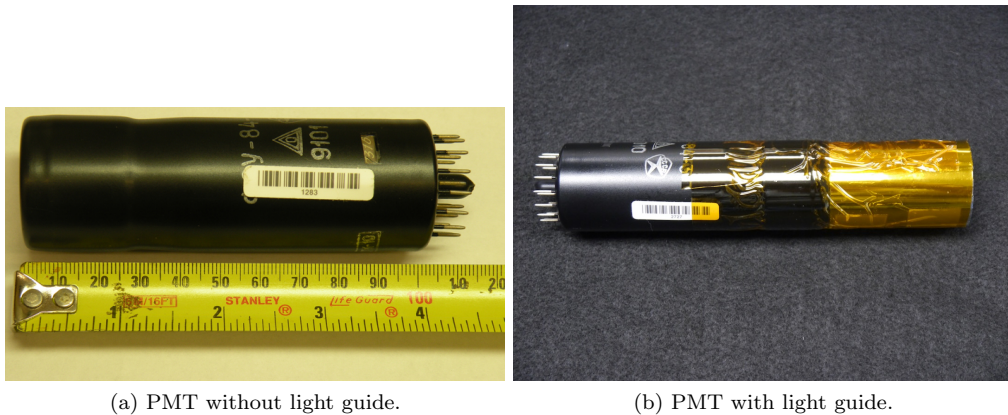


Figure 3: Pictures of a PMTs used in our measurements. The barcode and number can be seen on the sticker. The PMTs are of type FEU84-3 manufactured in Russia. The left picture shows a PMT before the light guide is glued on, while the right picture shows a PMT after the light guide is glued on.

2.2 Previous Measurements

Most of the PMTs had been tested before in 2005, and our first goal was to repeat those measurements and compare our results. The results of the previous measurements are kept in individual text files that recorded:

- the PMT ID
- the experiment that it was used in (E852 or RadPhi)
- iteration of measurement done, starting at 0
- the position of the PMT in the array that it was measured in
- for each PMT, the following were recorded over different high voltage settings:
 - total counts obtained
 - number of LED counts
 - aftercounts

Using a script, these measurements were read in and converted into ROOT graphs. There were a total of 4,002 measurements for the number of LED counts in coincidence as a function of high voltage (including duplicate measurements for the same PMTs), and Figure 4 shows an example of the previous measurements. The number of LED counts is shown as a function of the high voltage applied for each measurement. Details of the fit functions and analysis will be given in Section 3. Of the 4,002 PMTs, 1,074 were labeled as “RadPhi”, and 2,928 were labeled as “E852”. The old measurements were mostly done starting at a HV of 1400 V and went up to 1900 V in increments of 20 V.

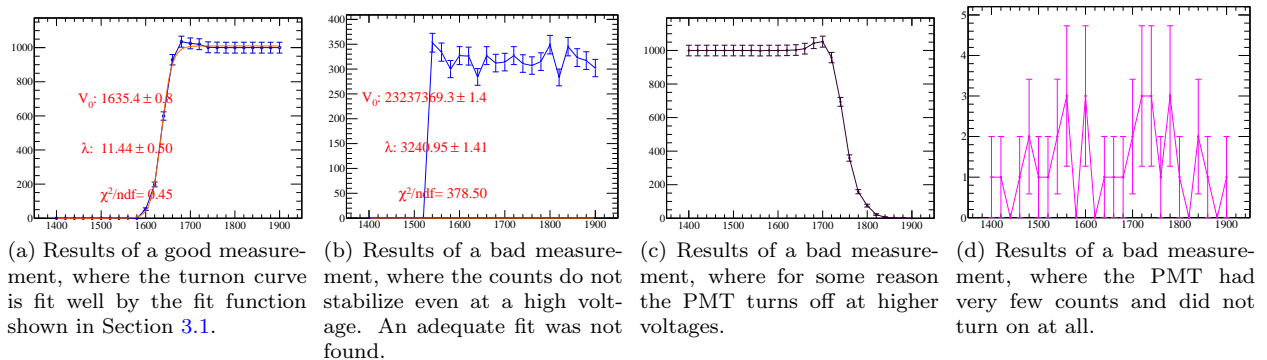


Figure 4: (a) shows the results of a good measurement done previously in 2005. The number of counts from the PMT in coincidence with the LED pulser are shown as a function of the high voltage that it was set to. (b)-(d) show examples of several different types of bad measurement where the PMT did not have a stable output.

2.3 Hardware

For our measurements, we placed the PMTs in a light-tight box with individual Cockcroft-Walton bases connected to each of them. The Cockcroft-Walton bases are the same type as the ones to be used in the final FCAL setup, and the firmware is currently being finalized. The high voltage on the PMTs were varied over a large range of 1200 to 2000 V, and an LED pulser was flashed within the box so that we could count the number of counts of each PMT as a function of high voltage, normalized to the LED counts. We call these measurements the “LED counts”, and these were the main focus of our measurements.

Also of interest were the so-called “aftercounts”, *i.e.*, the counts that were not in coincidence with the LED pulser. The reason for these counts can be difficult to determine, but some of the reasons include:

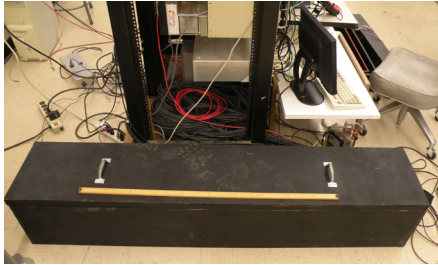
- noise being amplified by the high voltage
- damage to the PMT, such as bad vacuum, cracked cathode window, etc.

2.3.1 Dark Box

The measurements of interest were the LED counts and aftercounts as a function of high voltage for each PMT. The signals from each PMT were passed through to a discriminator, and electronics were used to form coincidences.

Figure 5 shows the light-tight box that was built to contain our setup. The dark box is made of wood, painted in black, and has outside dimensions of 164.6 cm (length) \times 33.0 cm (width) \times 30.4 cm (height). The wood used was of thickness 1.2cm, and made so that the lid could be easily opened, with the lid sliding in between two sets of walls to ensure light-tightness. Figure 5 shows some pictures of this dark box as well as a schematic of the box dimensions. The box can hold a maximum of 30 PMTs at once, stacked in five rows of six columns each.

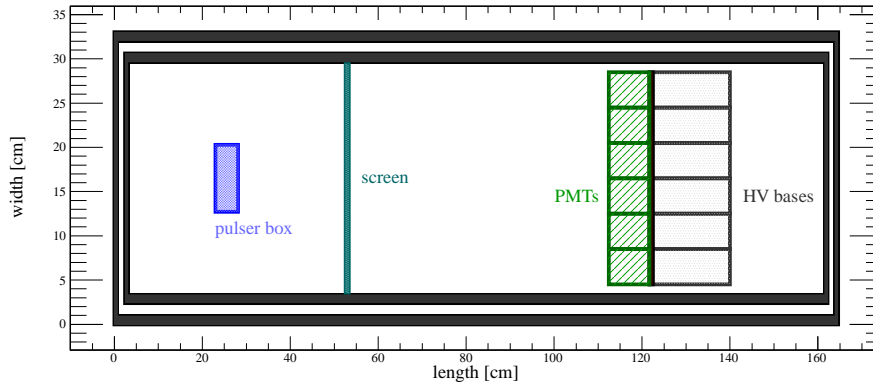
The box was tested several times for light-tightness by shining a flash light around the box and observing the signal from the PMTs. No change in the PMTs was observed.



(a) Outside view of dark box.



(b) Inside view of dark box.



(c) Schematic of inside of dark box.

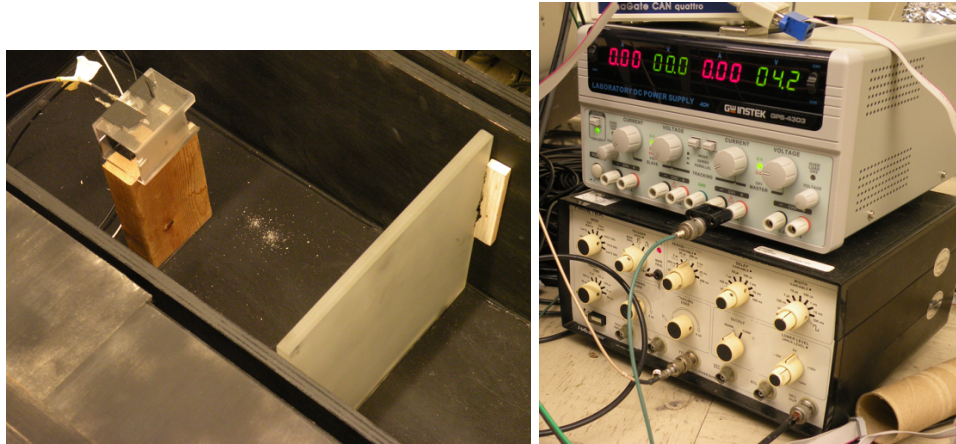
Figure 5: (a) shows the dark box from the outside along with a meter stick. (b) shows the dark box with the lid lifted. Inside we see, from left: the LED pulser on top of a wooden support, an acrylic board to scatter the LED light, the PMTs, high voltage bases. At the very right an interlock is seen that ensures that the high voltage does not turn on when the lid is open. (c) shows an approximate schematic of the inside of the dark box.

2.3.2 LED Pulser

The LED pulser used in our measurements was a custom made LED that was connected with two cables, one for supplying a voltage to accumulate charge, and the other for sending a trigger that would release the charge accumulated and light the LED. A picture of the LED and the supplies that handle the voltage and frequency of the LED are shown in Figure 6. The voltage on the LED was set at 4.2 V, and the frequency was set to 4 kHz (period 240 μs), with a signal width of approximately 100 ns. The light from the LED was then scattered using an acrylic screen, also shown in Figure 6.

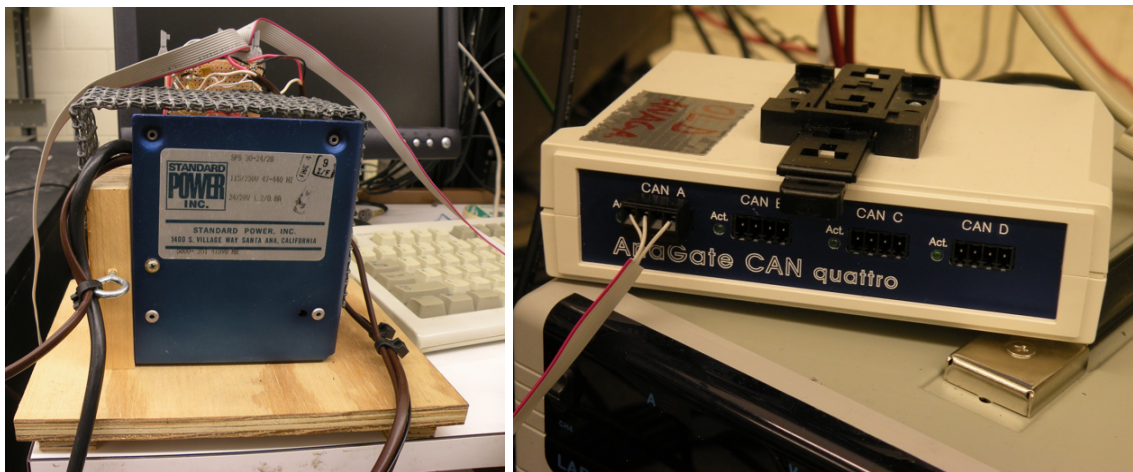
2.3.3 Voltage Supply

The voltage to the Cockcroft Walton bases was supplied by a voltage supply, which was coupled with a ANAGATE controller that was connected over an Ethernet connection. This ANAGATE controller is a prototype of the actual high voltage controllers that will be used in the GlueX Experiment, and pictures of the low voltage supply and controller are shown in Figure 7. Libraries supplied by the manufacturer were used to produce a program that controlled the high voltage.



(a) LED pulser, placed on top of wooden box (left), (b) Voltage and frequency controller of LED pulser and the screen used to scatter the light (right).

Figure 6: (a) shows the LED used in our measurements. (b) shows the voltage (above) and frequency (below) controller for the pulser.



(a) Voltage supply.

(b) ANAGATE voltage controller.

Figure 7: (a) shows the low voltage supply used in our measurements. (b) shows the ANAGATE voltage controller, which is communicated to via an Ethernet cable.

2.3.4 Barcode Scanner

Each PMT has a unique ID assigned to it, and this is labeled on each PMT both as print and barcode. Since we are interested in the characteristics of each individual PMT, the IDs were utilized. To efficiently read the IDs, a barcode scanner was used. This helped in reducing the time it took to read in the PMT IDs. Figure 3 shows the barcode on a single PMT and Figure 8 shows the barcode scanner.

One thing to note about the barcode reader is that, while it is highly reliable and efficient to use, we did notice that sometimes the barcode reader misreads the barcode. There were at least three cases where the barcode was misread, as shown in Table 1. In the actual reading in of the barcodes during installation, a program will be set up with the ability to discriminate in cases where the barcodes shows non-numeric values. It should be kept in mind that the barcode reader will fail with a probability of $\sim \mathcal{O}(1/1000)$.



Figure 8: The barcode scanner used to read in the PMT IDs efficiently.

actual barcode value	read in value	note
6283	628z	Found due to non-numerical ID.
6459	6419	Was caught due to PMT being part of contiguous run of IDs.
1513	1e13	Found due to non-numerical ID.

Table 1: PMT IDs that were misread by the barcode reader. Of the ~ 3300 tested, at least three cases were found where the barcode reader failed.

2.3.5 Electronics

To read out the signals from the PMTs, electronics were heavily used. Our setup used the following electronics:

- CAMAC modules
 - 2 Phillips 7106 discriminators (16 channels each)
 - 2 LeCroy 4434 Scalers
 - 2 IU custom-made coincidence units to read in two 16 channel ribbon cables and take a coincidence with a separate channel. The total of 32 channels available in these modules were the restriction on how many PMTs we could test at once.
- NIM modules
 - Phillips 726 ECL/NIM/TTL translator
 - cable delay
 - Phillips 794 quad gate/delay generator
 - Yale 124 fanout

The timing and logic of the setup is shown in the next section.

2.4 Signal, Timing and Electronics

The electronics diagram for the setup is shown in Figure 9. The pulse generator sends out a signal at constant intervals, sending the TTL signal to the LED, while the other signal is sent to the NIM logic setup for timing delays and gates. The logic signal is converted to a NIM signal using the Phillips 726 signal translator (channel A), and then split into two, one for the LED signal, and one for the aftercounts. The LED signal has a short delay, so that the signals will have the same timing as the signals from firing PMTs, which take time to form. The LED signal is split into two, and one signal will go directly into the discriminator for LED counts, while the other signal is gated for 50 ns for a coincidence window for LED counts. The aftercounts signal, after being split from the LED signal, will be passed through a delay and then gated for 10 μ s for the aftercounts coincidence window. Any PMT pulses that are in coincidence with this window are counted as aftercounts.

Meanwhile, the signal from the pulse generator will generate a flash of the LED, causing the PMTs to fire. The signals from the PMTs will be passed into a discriminator, along with the formatted LED signal. After being discriminated, the signals are each ANDed with the gates for LED signals and aftercounts. Each result of the AND operation is then passed into a LeCroy 4434 scaler, and counts are taken.

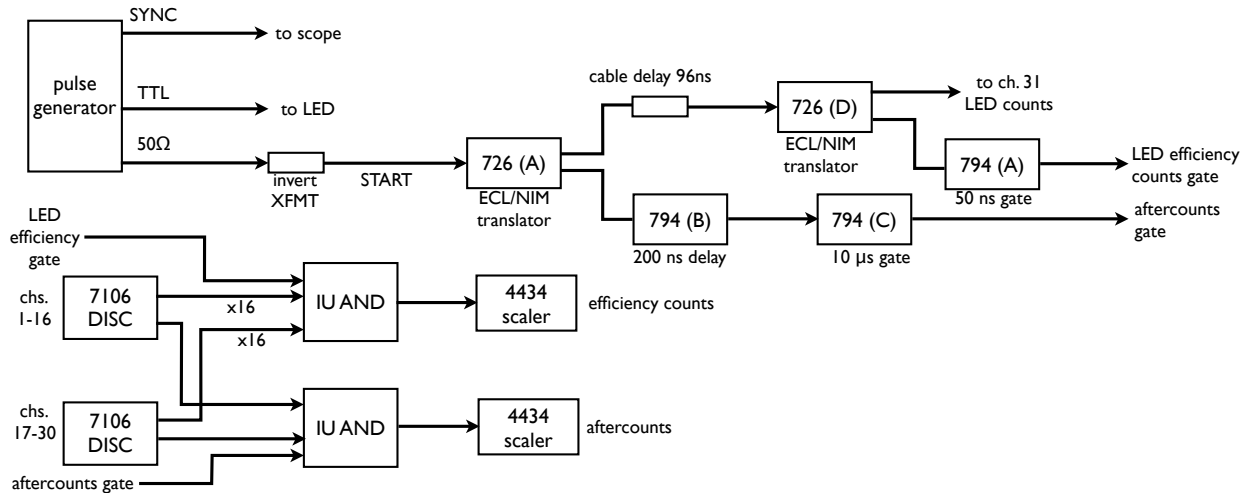


Figure 9: The electronics logic used in our setup. The numbers within the boxes show the component names, with the channel used in parantheses, while the captions underneath show what the effect is.

Figure 10 shows the timing of the electronics. In this example, the gates for the LED signal and aftercounts are shown by the dashed red and blue lines, respectively. If the PMT has a signal within each window, the scaler will add a count for each respective count.

2.5 Programs Used

Programs were written to automate our measurements. The main program was called `PMTtester2`, written in C++, with commercial libraries provided for the high voltage controller. The output of this program was a ROOT file that contained a TTree containing all the measurement results, as well as run information, such as date and threshold values. A program for the barcode reader called `barcodeReader`, written in C++. After measurements were made, the results could be displayed and analyzed quickly with the ROOT macro `createPlotsMacro2.cc` which took the current run number as an argument.

The above programs were installed on the machine `mantrid01` which was connected to our setup, but for a more detailed analysis, the output ROOT files were transferred to `/home/s4/kmoriya/PMT/PMT-HV` on

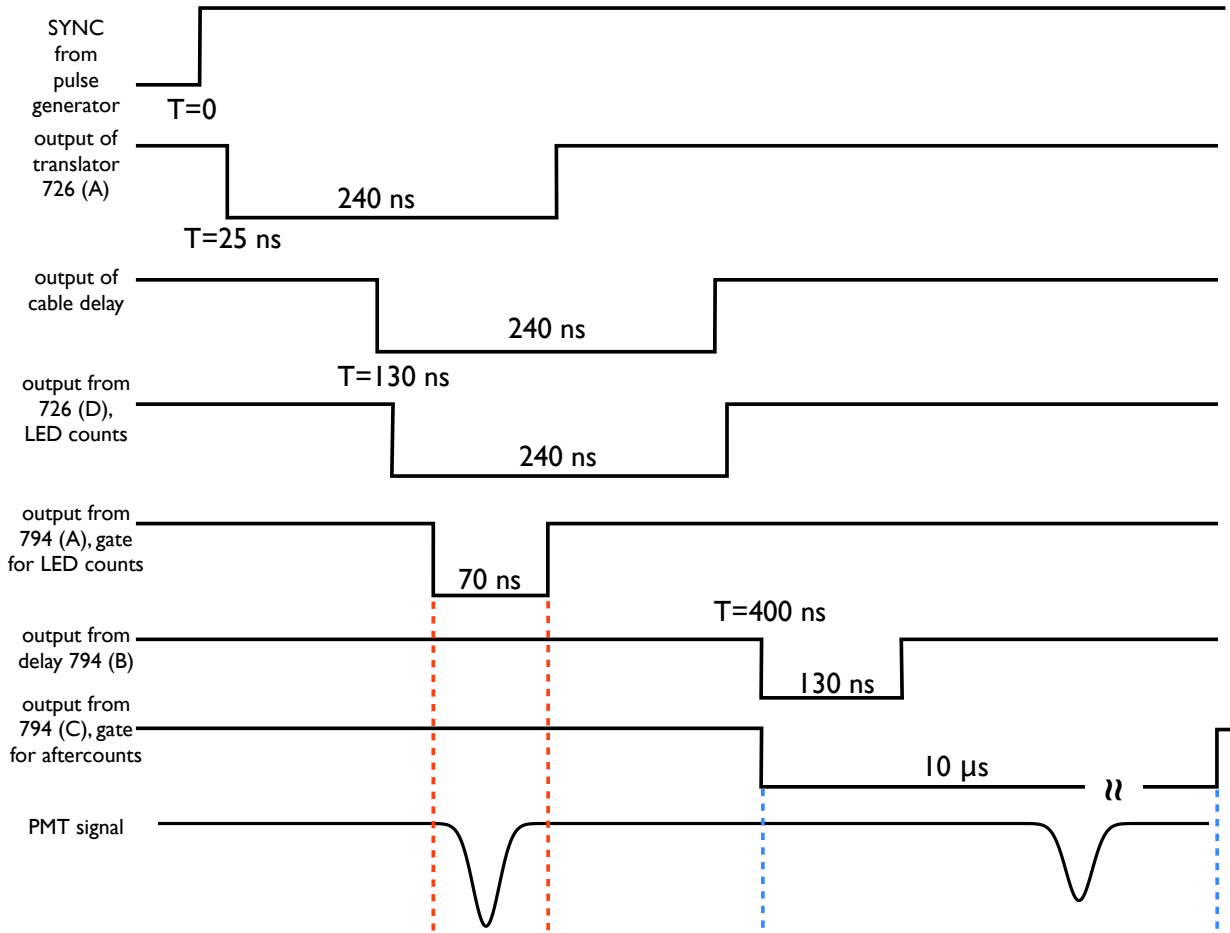


Figure 10: The timing of electronics logic used in our setup.

the IU Task-D system, and analyzed with the program `xCreatePlots2`, written in C++. The details of the measurements and how they were saved and analyzed will be shown in the next section.

3 Measurement Results and Analysis

In this section we will analyze the data that was taken for each measurement. The data were compressed as ROOT files, and ROOT executables were used to efficiently read out and analyze the data. We start with our main focus, the LED counts, and then analyze the aftercounts.

For each PMT, measurements were done by changing the HV value between 1200 V and 2000 V, starting at 2000 V and decreasing by 8 V for each measurement. The measurements were repeated over five different discriminator thresholds, so that we would have a measurement of how the PMT output changed with voltage. These measurements were all done in one run, so that the final ROOT file had all of this information for up to 30 PMTs.

3.1 LED Counts

The LED counts data were fit to a function of the form

$$f(V) = \frac{C}{(1 + \exp[-(V - V_0)/\lambda])}, \quad (1)$$

where V is the value of the high voltage, and the three fit parameters are

- C – overall normalization of counts
- V_0 – central value of high voltage where PMT turns on
- λ – characteristic scale at which PMT turns on.

As can easily be seen, the fit function has a value of $C/2$ at $V = V_0$, and asymptotically approaches $0(C)$ as $V \rightarrow 0(\infty)$, with a characteristic change of scale λ .

A good PMT will give a good fit to this function, as was illustrated in Figure 4a from previous measurements. The previous measurements from several years ago were also fit to this form.

It was noticed that the value of V_0 had a rather significant shift depending on how long it had been since the PMT had been initially powered up, probably due to settling of the PMT. As we are interested in the PMT behavior after it has been powered up for a long time, we decided to have a two hour delay before measurements. The PMTs were all held at a constant voltage of 1500 V for two hours before starting the measurements.

Figure 11 shows an example of a measurement of the LED counts. The 30 PMTs are shown, as well as the LED pulser signal. All signals are seen to turn on at a HV value between 1200 and 1500 V. We noticed that for some of the PMTs, the signal did not always saturate at the LED counts at high HV values, but rather had a falloff in efficiency. This was found to be due to the aftercounts coming in at such a high rate that the discriminator did not have enough time to recover. As we initially did not know what the reason for this loss in efficiency was, we decided that these PMTs would be retested (see Section 3.2).

Figure 12 shows the PMT HV as a function of discriminator threshold. We can fit the PMT behavior as a function of threshold with the form

$$V_0(t) = Ae^{t/B}, \quad (2)$$

where t is the discriminator threshold in mV, and V_0 is the turnon HV value in V. The motivation for this form is due to the output signal being roughly proportional to the number of dynode divisions in the PMT, and inverting the relation. A polynomial fit was also tried, but gave a worse deviations at higher voltages than the power function, so was not used. The fit functions may be useful if in actual GlueX data taking, it is decided that the PMTs should have a minimum threshold of several hundred mV, as this fit allows us to extrapolate to find the HV setting necessary. The values of λ were found to be largely independent of the threshold values used.

Each of the good PMTs tested gave a value of 900–1100 and 11–15 for the fit parameters A and B respectively, and are rather consistent with our assumption with the shape. Figure 13 shows the distributions of the fit coefficients A and B .

In all, 2436 PMTs had measurements that we deemed were good, and needed no further testing. The PMTs that had a falloff in efficiency were retested.

3.2 Retest

For the retesting of PMTs, we did multiple measurements over the course of several days. Each retest was done two hours after the previous measurement, with the HV kept at 1500 V in between measurements. The duration of each measurement is about 1 hour and 45 minutes. It was found that with several measurements, almost all of the PMTs that we retested no longer showed the loss in efficiency, probably due to the settling down of the PMT.

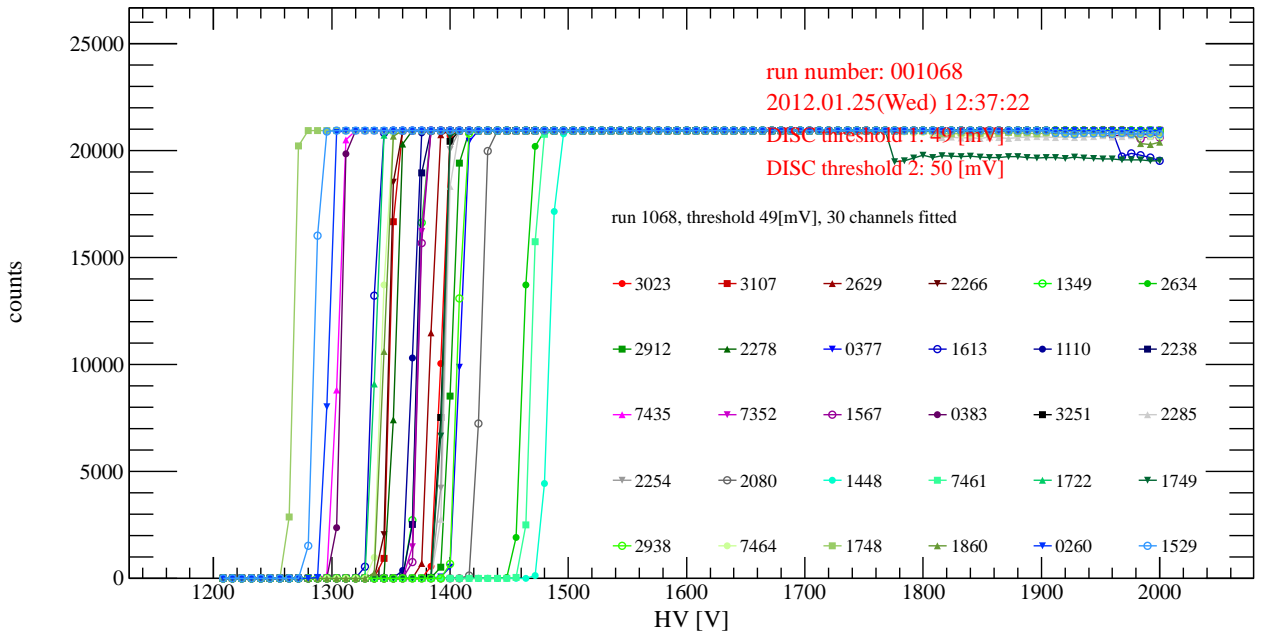


Figure 11: An example of LED counts for 30 PMTs, taken with a discriminator threshold of 50 mV. The number of LED counts that were in coincidence with the LED counts window are shown. Note the falloff in efficiency at high HV values for several of the PMTs.

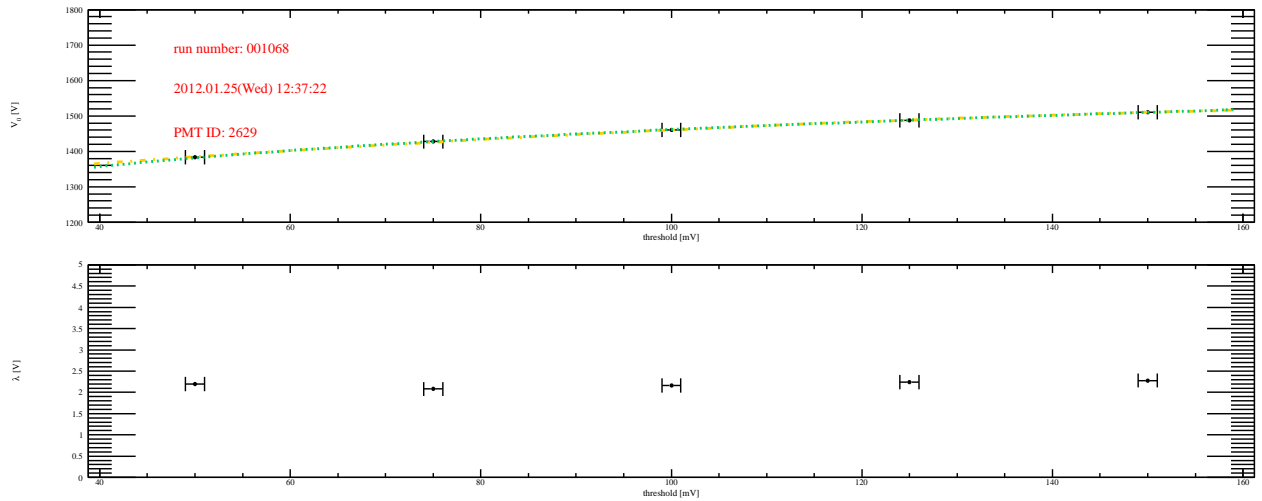


Figure 12: The behavior of the fit values of V_0 (top) and λ (bottom) against the discriminator threshold for a given PMT. The two fit curves for V_0 show a fit with a power function (teal) and a second order polynomial (orange).

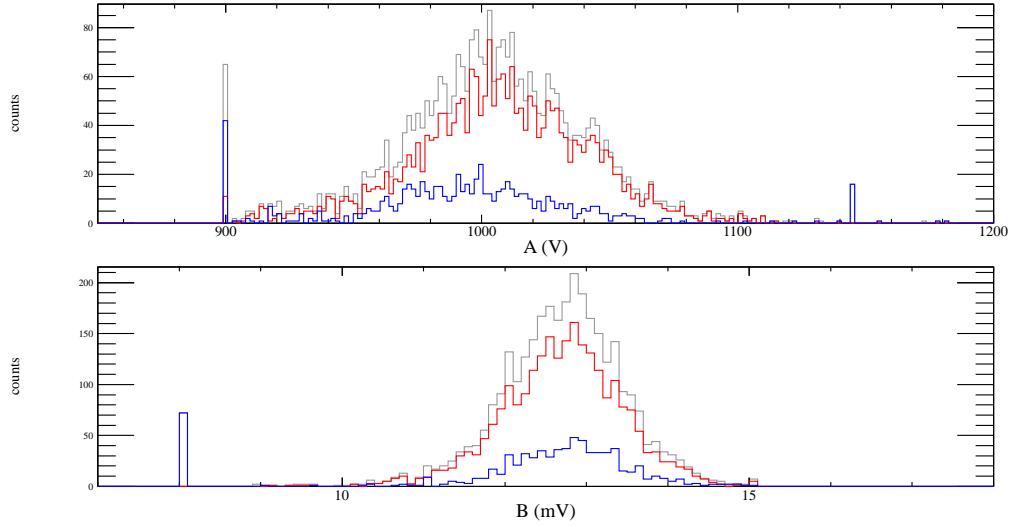


Figure 13: Distribution of fit coefficients A and B from Eq. (2). The gray histogram is for all PMTs, the red histogram is for good PMTs, and the blue histogram is for retested PMTs. The spikes at the edges are due to our restricting the fit parameters to that range.

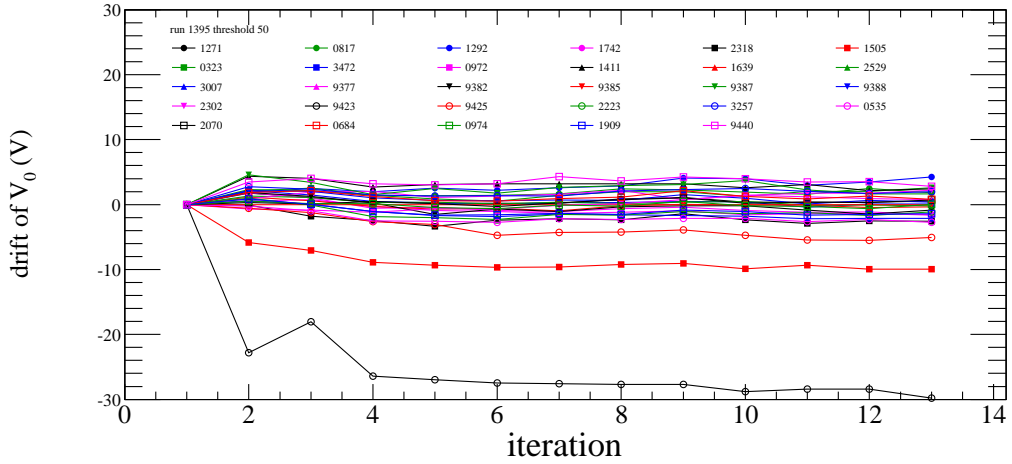
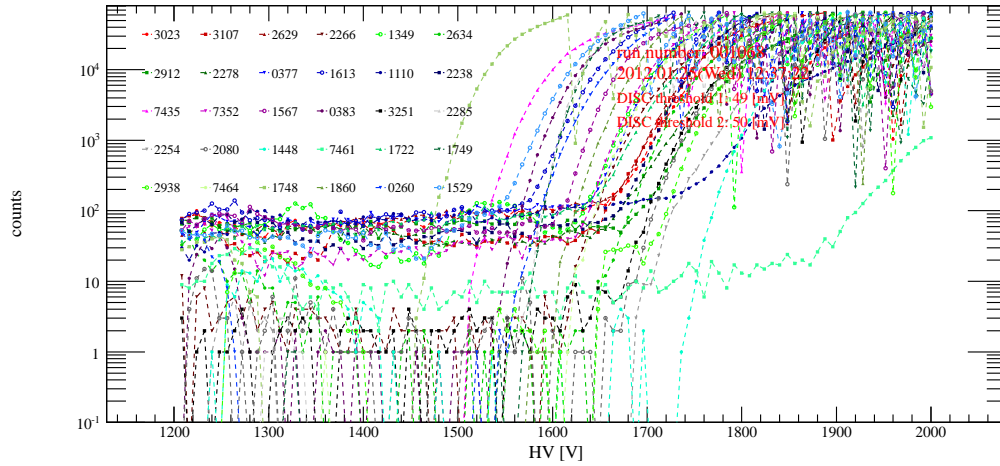


Figure 14: The behavior of the fit values of V_0 against the retest iteration number. Each retest is done approximately 3 hours and 45 minutes apart. PMT 2070 is seen to have a very large drift of V_0 compared to the other PMTs.

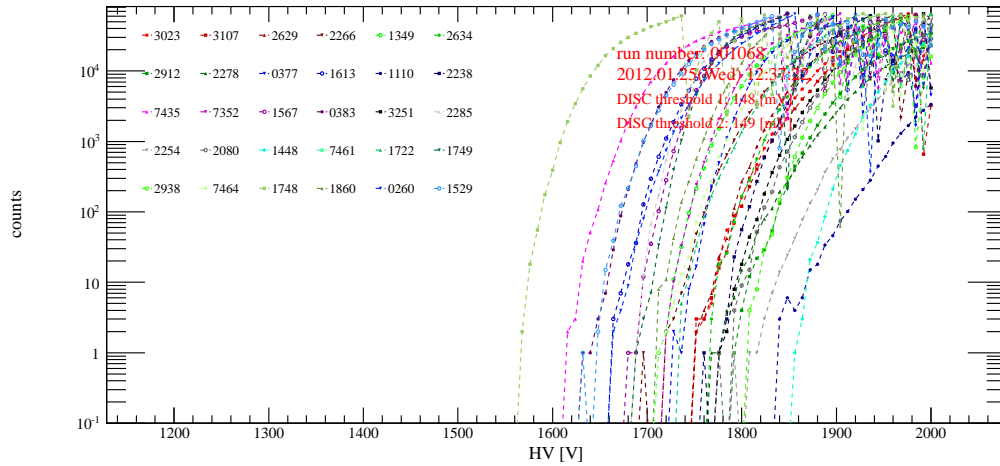
The values of V_0 were observed as a function of time, and it was noticed that for some PMTs, there was a sizable drift in the value. For most PMTs, the drift was less than 10 V, but for some PMTs, values as large as 30 V were observed. As this signaled an aging or bad PMT, we decided that this would be the criteria for which to remove PMTs. Figure 14 shows the change in V_0 values of each PMT as a function of iteration, where the initial measurement of V_0 is set as an offset. Each iteration was taken approximately 3 hours and 45 minutes apart, and we see how as time progresses, the values of V_0 change. For most PMTs the change is within a ~ 8 V, but for some PMTs the changes exceed 10 V. The drift in V_0 was one of the criteria that we used in selecting the final PMTs to be used in the GlueX setup, and this is described in Section 5.

3.3 Aftercounts

For the aftercounts, typical measurements looked like Figure 15. The signal size of the aftercounts are rather small and show most prominently at a threshold value of 50 mV, but at high HV values, show up even with a threshold value of 150 mV.



(a) 50 mV



(b) 150 mV

Figure 15: Aftercounts for each of the 30 PMTs tested for a single run for the smallest (top) and largest (bottom) discriminator thresholds.

The aftercounts are the counts that are out of coincidence with the LED, and the counts are integrated over the measurement period of approximately 2 s, with each period being $240\mu\text{s}$. For each LED cycle, the aftercounts are counted within a window of $10\mu\text{s}$, which is much longer than the coincidence window of 50 ns that we used for the LED counts. Therefore, it is not possible to directly compare the absolute counts of the LED counts and aftercounts, but since all of the aftercounts for each PMT were measured in the same way, we can make a comparison of the number of aftercounts for each PMT. We also note from Figure 15 that, as the scaler we used only has a maximum value of $2^{14} - 1 = 16,383$, for measurements when the aftercounts exceed this value, an overflow occurs and we see drops in the aftercounts at higher HV values.

As high aftercount rates signal an aging PMT, PMTs that had extremely high aftercounts rates at low

HV values were also removed as part of our criteria in selecting the final PMTs for GlueX.

3.4 Correlations with Previous Measurements

Now that we have fit the previous measurements and our current measurements with the same form, we can do a comparison. Since the setups are not exactly the same, comparing the values of V_0 and λ directly is meaningless. However, we do expect there to be a strong correlation between the previous values and the current measurements.

In all, of the 4002 previous measurements, there were 2498 unique IDs. In most cases the fits were not even tried as the PMT turned on before the lowest HV value of 1400 V (1789 times), so that there were only 2213 measurements where a fit was attempted. Of these, 2213 had a successful fit, while ~ 7 measurements did not converge after 500 tries, and 2206 measurements converged. Of these 2206 that converged, there were 1687 PMTs that had one good measurement, 212 that had two good measurements, and 20 that had more than three good measurements.

The criteria for selecting the old measurements was that

- the LED counts at the lowest HV value was less than 100
- the fit converged within 500 tries, with $\chi^2/\text{ndf} < 10$, $500 < V_0 < 3000$, and $\lambda < 1000$ (very loose cuts)
- there were no duplicate measurements of the same PMT that met all the criteria above

The reason for the final criteria is simply because we do not know which measurement to trust, as the values were in many cases not consistent with each other. Therefore, our final sample was 1687 old PMTs, and for these PMTs, the new measurements done at a discriminator threshold of 50 mV was compared.

Figure 16 shows the distribution of V_0 and λ that were obtained in the previous measurements. The λ value is much more spread out than our current measurements. This is probably due to the old measurements having high voltage increment of 20 V, much more than the λ values, which would lead to an imprecise determination of λ . Figure 17 shows the correlation of the fitted V_0 values for the old and new measurements. As expected, a correlation is seen between the PMTs, although the conditions for the measurements could have been rather different, and the time between the measurements was several years.

Our conclusion here is that the V_0 values for the PMTs do not change rapidly over time, and within the systematics of the measurements, they are highly correlated.

4 Systematics of Measurements

There are several sources of systematic errors to be considered in our measurements. The first is the actual voltage set on the PMT bases, as opposed to the voltages that they were set to. Dan Bennett did a study on eight bases, where the high voltages (HV) values were read out directly on a tester, instead of on the internal ADC, where the resolution is worse. The results are shown in Figure 18, and we see a very nice correlation between the set values and actual values.

The average values, standard deviations, and absolute values of the shifts for the eight bases that were tested are shown in Table 2 for the nine different HV values that were tested. Note that these values include the errors on the resistor that was used in the measurement (several resistors accurate to 1%). The systematic error on the actual HV value is seen to be on the order of 5 V.

In Section 5, we will see that there is a difference in the distributions of V_0 depending on the 30 channels that were used for measurements, and we will try to correct for the differences between channels so that the centroid of each channel's distributions is set to the same value.

Another source of systematic error is in the drift of the PMT behavior with time. As the PMTs take some time to settle, the values that we extract for V_0 and λ also drift. This will be seen in Figure 14, where the drift is used as a criteria for selecting the final PMTs to use. As was mentioned before, To eliminate most of this behavior, in all tests the HV values were kept constant at 1500 V for two hours prior to the measurements.

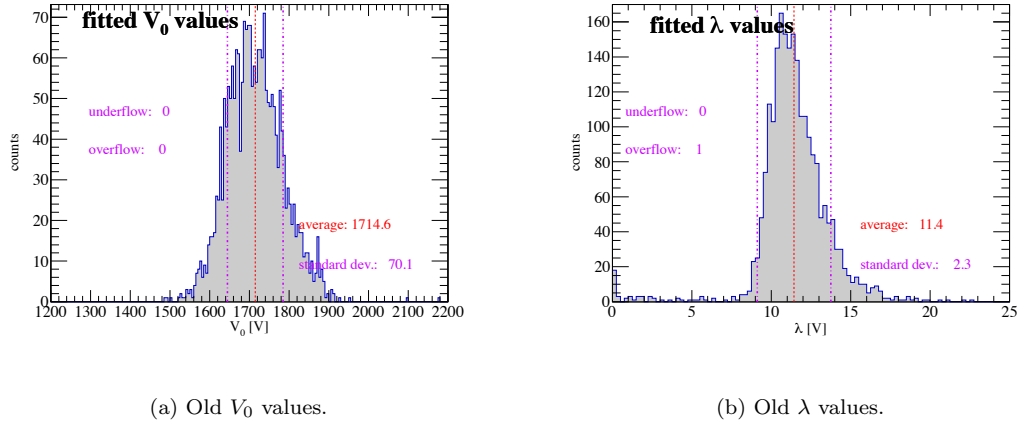


Figure 16: (a) shows the distribution of V_0 (V) from previous measurements done several years ago. (b) shows the distribution of λ (V). The λ distribution is hampered by the fact that measurements were only done at 20 V increments.

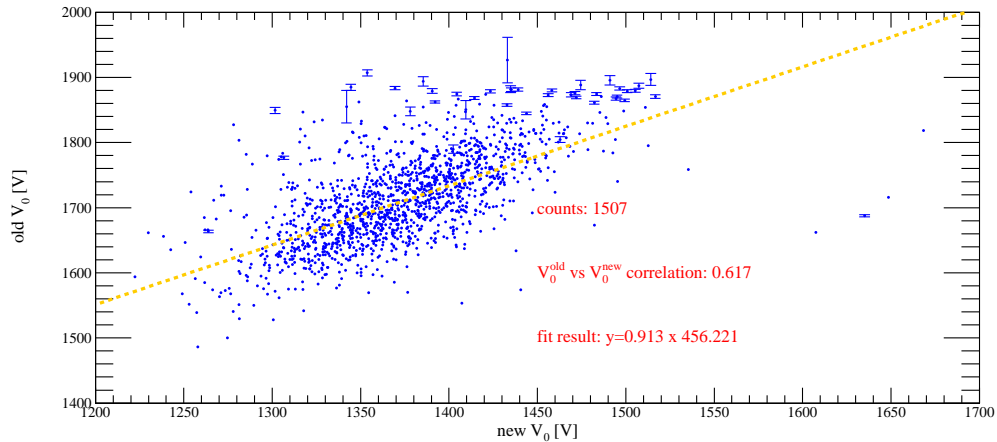


Figure 17: Correlation of the old measurements and the new measurements done with a discriminator threshold of 50 mV. A rather strong correlation is seen between the ~ 1500 measurements that were included in both datasets.

4.1 Comparison of Subsets of Data

The data that was taken can be divided into various subsets, such as what kind of PMT it was or when the data was taken. As previously mentioned, most of the PMTs were used in past experiments E852 at Brookhaven and RadPhi in Hall B of Jefferson Lab. Apart from these “old” PMTs, ~ 440 “new” PMTs were newly acquired around 2010. Figures 19 and 20 show the V_0 and λ distributions for the old and new PMTs, respectively. We see that under the same test conditions, the old and new PMTs show remarkably similar behavior, and for at least the gains, there is no quantitative difference.

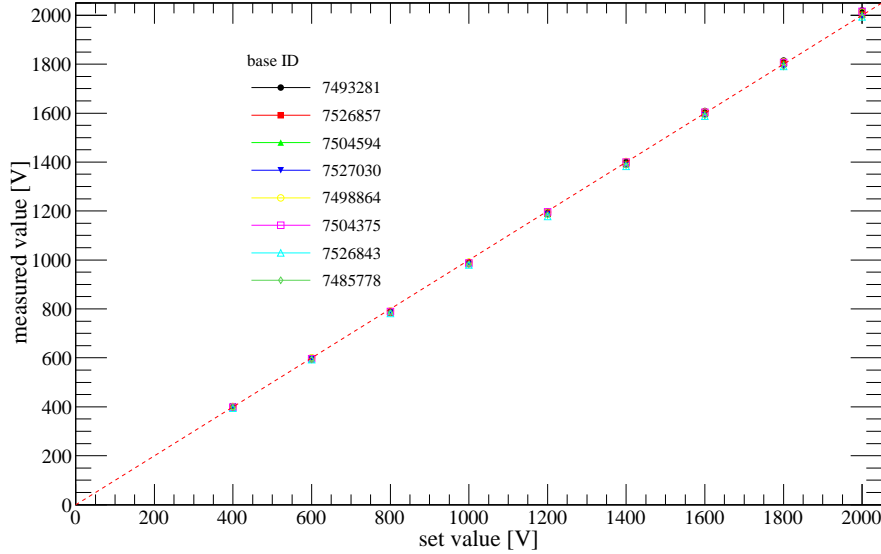


Figure 18: Measurements of HV against set values for eight different bases. The measured voltages are almost perfectly aligned with their set values.

set value	average (V)	standard deviation (V)	shift (V)
400	399.625	2.9128	0.375
600	595.875	2.89126	4.125
800	787.25	3.59687	12.75
1000	985.5	4	14.5
1200	1190	6.2849	10
1400	1393.75	6.79614	6.25
1600	1597.88	7.02562	2.125
1800	1801.12	8.78119	-1.125
2000	2004.62	10.0242	-4.625

Table 2: Average, standard deviation, fractional errors for measured high voltages on eight bases. The shift is given as $|\text{average} - \text{set value}|$.

5 Criteria for Selection of PMTs

Based on our measurements, we selected the 2,800 PMTs necessary for the GlueX FCAL. In total, we started with approximately 3,300 PMTs, and removed 58 that were clearly broken. Of the ones that remained, we determined that approximately 3,100 were useable in the final setup. As the final GlueX setup requires only 2,800 PMTs, and we found that some PMTs have unwanted characteristics such as high aftercounts and drifts of V_0 , set up a list of criteria for selection.

Our final criteria was based on three requirements,

1. the V_0 values were not outliers within the distribution
2. for the retest PMTs, the drift of V_0 was not significant
3. the aftercount rate was not high

We start with 2497 PMTs that were singly tested with no retest, and 711 PMTs that were retested. Below we explain how each cut reduces the number of PMTs, and our final selection criteria. The PMTs will

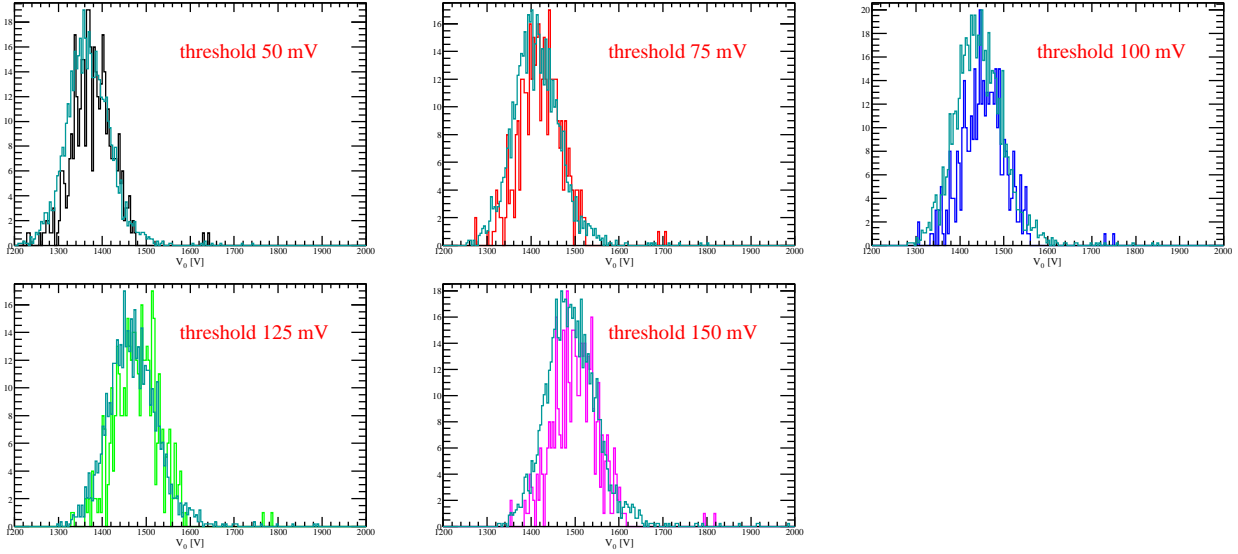


Figure 19: Comparison of V_0 from old and new PMTs. There are roughly 2700 old PMTs from E852 at Brookhaven and RadPhi from Hall B of JLab, and 400 new PMTs that were newly acquired. The distribution for V_0 looks very similar. The different panels show the measurements done at different discriminator thresholds, and the histograms in light blue show the new PMTs. The distribution of new PMTs have been scaled to have the same height as the old PMT distributions.

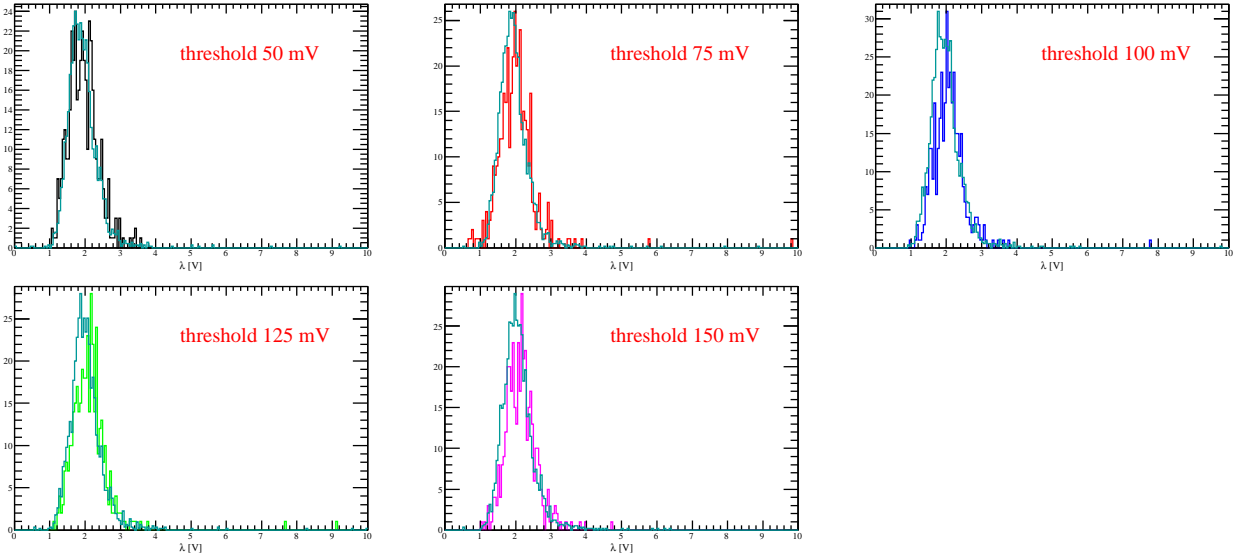


Figure 20: Comparison of λ from old and new PMTs. The distribution of new PMTs have been scaled to have the same height as the old PMT distributions.

be given a status of “good”, “bad”, “retest”, and “spare”, depending on how their measurements were. The final PMTs that will be used will be the “good” and “retest” ones, while the “spare” ones will be used if we run out of the previous two. To ensure that we have a uniform distribution of the quality of PMTs across the entire FCAL, no selection will be made of the PMTs depending on the position within the detector. As the

final number of PMTs that were “good” and “retest” were 2436 and 463, respectively, during installation, for every five “good” PMTs, a “retest” PMT should be inserted.

5.1 V_0 outliers

The majority of the PMTs are singly tested PMTs that were deemed unnecessary to retest. Among these, we want to eliminate PMTs that have very different V_0 values compared to the others, as this will cause a large difference in gain, if set to similar high voltage values.

Figure 21 shows the distribution of V_0 for each threshold measurement. It was noticed during analysis of the PMTs that there was a channel-dependence of the central values of V_0 when the distributions of each channel were fit individually. The reasons for this are not entirely clear, but there are several possibilities, such as

- LED luminosity depending on the position of the channel within the setup
- differences in bases used

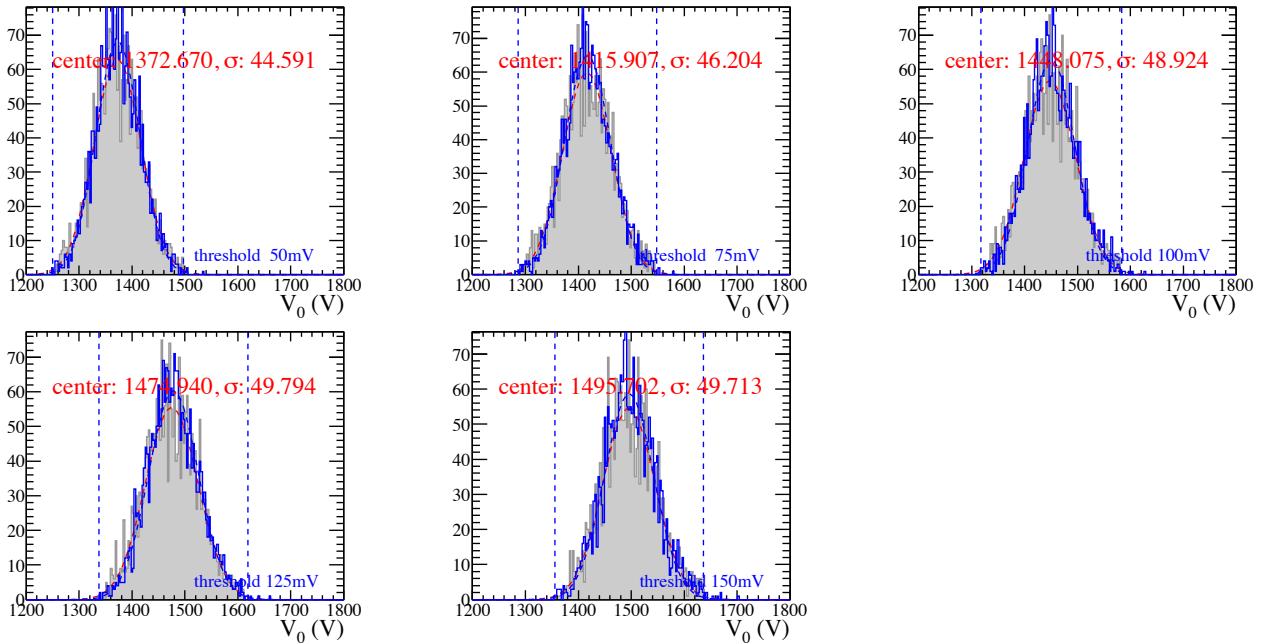


Figure 21: V_0 distributions for each threshold. The gray histograms are the raw measurements done, with the red dashed lines showing the Gaussian fit curves. The blue histograms are after channel-dependent corrections, with blue dashed lines showing the Gaussian fit curves.

For each threshold, the distribution of V_0 was fitted with a Gaussian function, both for the overall distribution and for each channel independently. Within Figure 21 the channel-dependence-corrected distributions are shown as the blue histograms, and the fits are shown as red dashed lines. The results of fits to the V_0 distributions for each channel are summarized in Figure 22, where the central value of the fitted Gaussian function is shown against channel number.

To remedy the channel-dependence, the V_0 values of each PMT was scaled by a factor of

$$c_i = \frac{\langle V_0 \rangle}{\langle V_{0,i} \rangle}, \quad (3)$$

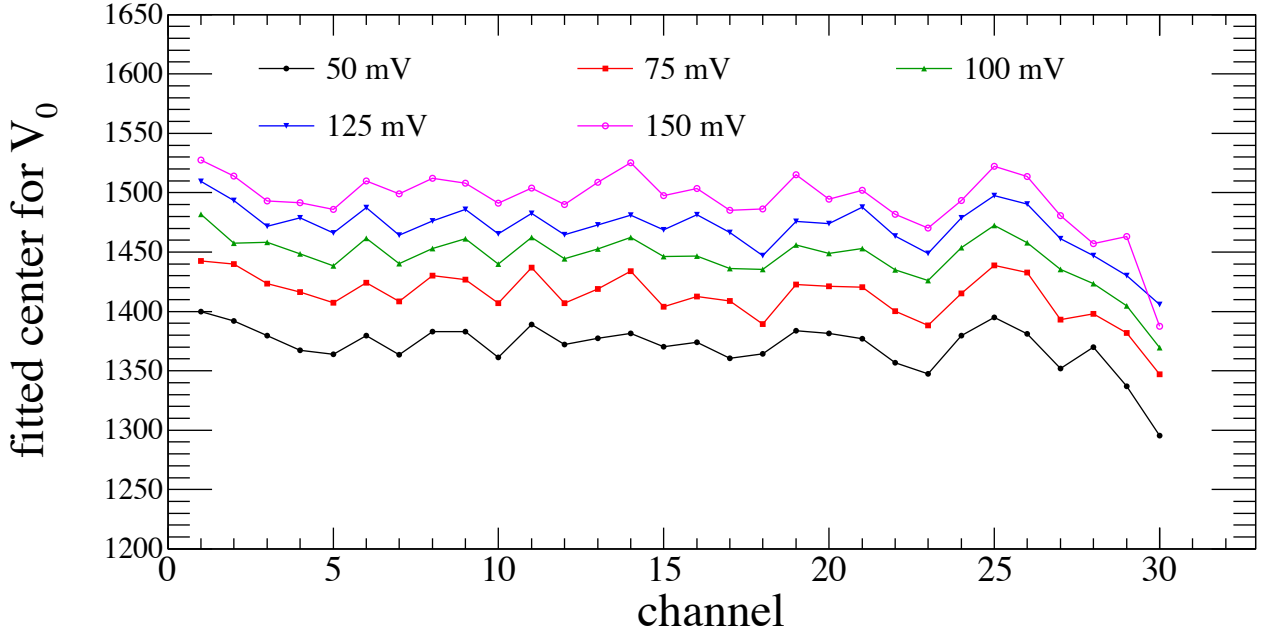


Figure 22: V_0 distributions for each channel. Each color represents a different threshold measurement. The values are the centroid of V_0 when the distributions of V_0 are measured for each channel independently.

where $\langle V_0 \rangle$ is the overall central value using all channels, and $\langle V_{0,i} \rangle$ is the fitted central value of the channel i that the PMT was measured in. Once we have the corrected distribution of V_0 values, we can remove the outliers by removing the PMTs that had a value outside of the $\pm 3\sigma$ range of the fitted function. We find that for the singly tested PMTs, 43 PMTs are marked as “spare” in this way.

The distributions of V_0 were looked at for the retested PMTs also, and we used the same boundaries of $\pm 3\sigma$ based on the good PMTs to select ones that were outliers. The result was that there were 7 PMTs that had V_0 consistently outside of that range, and these were also marked as “spare”.

5.2 High aftercounts

For all PMTs, we want to avoid the use of PMTs that have large noise, as these will interfere with real signal in the experiment, and also indicate aging of the PMT. Here we explain the criteria that was used to remove such PMTs.

In Figure 15, it was seen that all PMTs have counts that are out of coincidence with the LED pulser, which we call aftercounts. All PMTs show some kind of aftercounts, but the HV at which they become prominent depends on the PMT. Since the curves shown for each PMT increase monotonously, we can select an arbitrary number of aftercounts and see where the aftercounts exceed that value. We chose a value of $N = 10,000$ as our criteria, and Figure 23 shows the HV value at which the aftercounts exceed N . The gray histograms are for all PMTs that were tested, including the ones that were retested, the red histograms show the distribution for PMTs that were only singly tested, and the blue histograms are for PMTs that were retested. We see here that the retested PMTs have a very strong tendency to have high aftercounts at lower HV values than the singly tested ones, and this lead to the loss of efficiency at high HV values.

Figure 24 shows the cumulative distribution of PMTs that exceeded N aftercounts at a given HV value. The black graph is for all PMTs, and the blue curve is for PMTs that were retested. We see that the PMTs that have high aftercount rates at lower HV values are dominated by the ones that were retested. Also, for the retested PMTs, we see that there are ~ 200 PMTs that have a high aftercount rate below 1600 V, but beyond that, almost all PMTs will have a high aftercount rate. Therefore, we decided to remove PMTs that

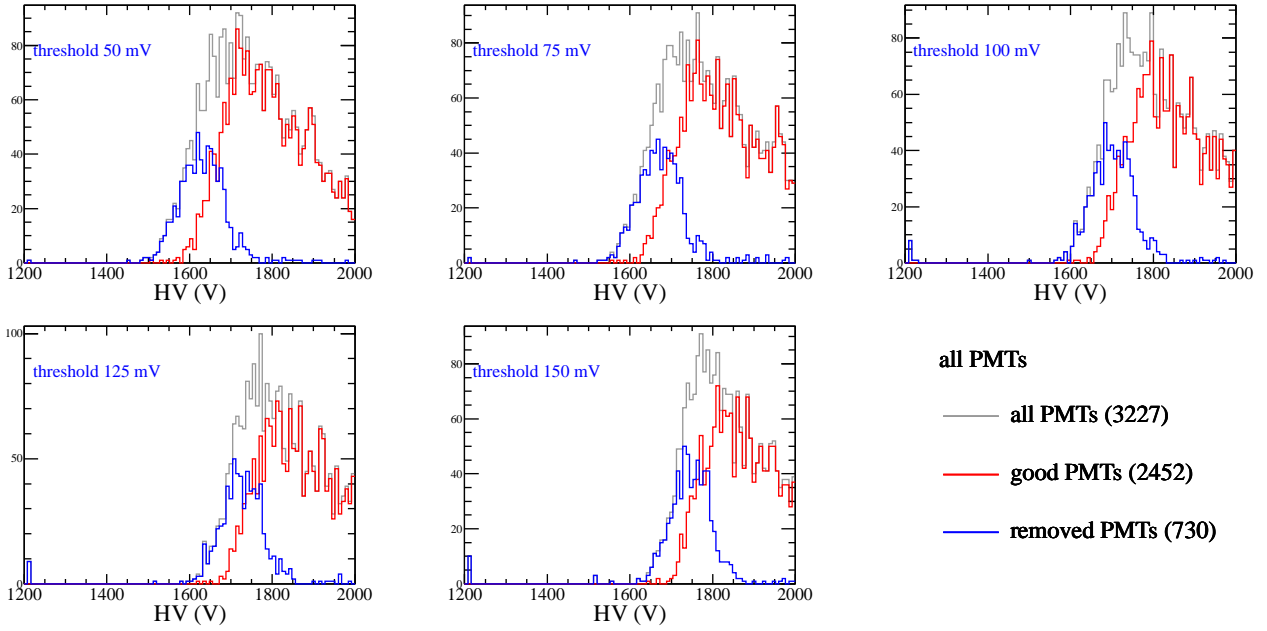


Figure 23: Distribution of HV values at which each PMT had an aftercount of higher than 10,000 counts. Each panel represents a different threshold for the measurement. Our criteria to select PMTs (Section 5) uses only the measurements at 50 mV.

had high aftercount rates below 1600 V. This lead to marking 16 PMTs within the singly tested PMTs, and 186 PMTs from the retested ones as “spare”.

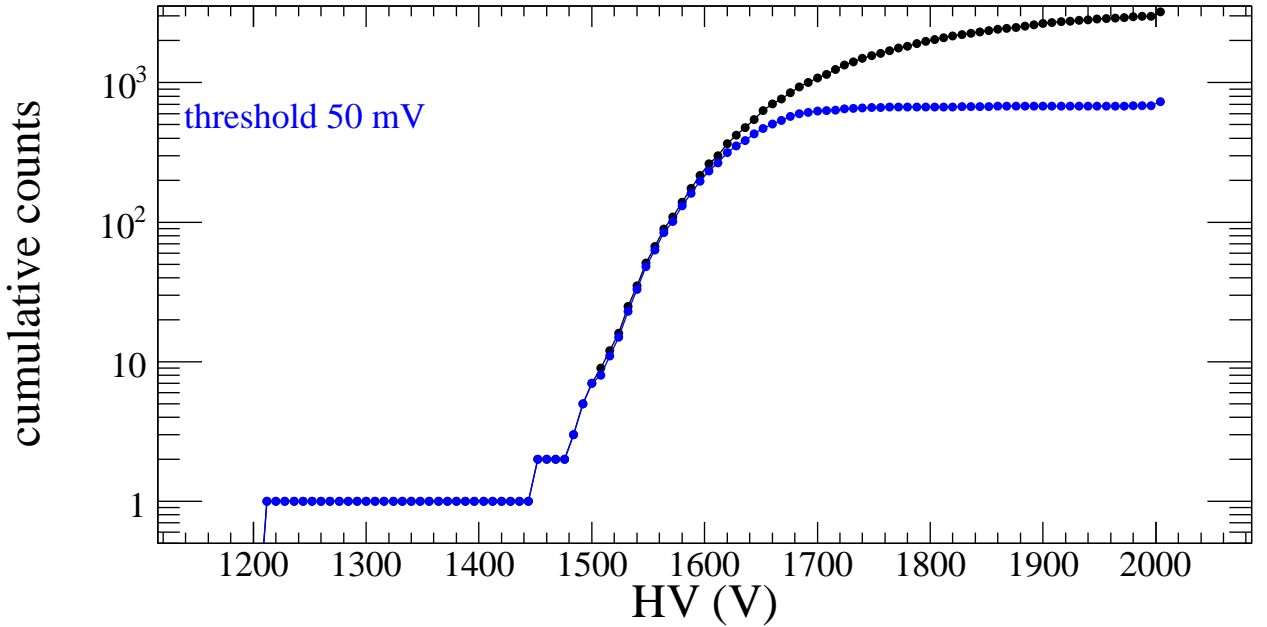


Figure 24: Cumulative counts of PMTs that had more than 10,000 aftercounts for a given HV value. The black points are for all PMTs tested, while the blue points are for the retested PMTs.

5.3 Large drifts in V_0

Our final selection is for the PMTs that had a large drift of V_0 against time. In Figure 14 we saw that some PMTs that were retested had a drift of V_0 between measurements that exceeded 10 V or more. Since this is an unwanted characteristic, we remove PMTs with large drift values. Figure 25 shows the distribution of the final drifts that we observe during retesting. Note that for each set of retests, the number of iterations is not constant, but varies between 11 and 20. However, as seen in Figure 14, most of the drift occurs during the first several runs, and the drift values are much less as we iterate.

From Figure 25, we see that there are several PMTs that have large drift values, but most of the PMTs are clustered in the middle with drift values of less than ~ 8 V. Therefore, we remove only PMTs that have a drift of more than 8 V, and this removes 22 PMTs from the retested PMTs.

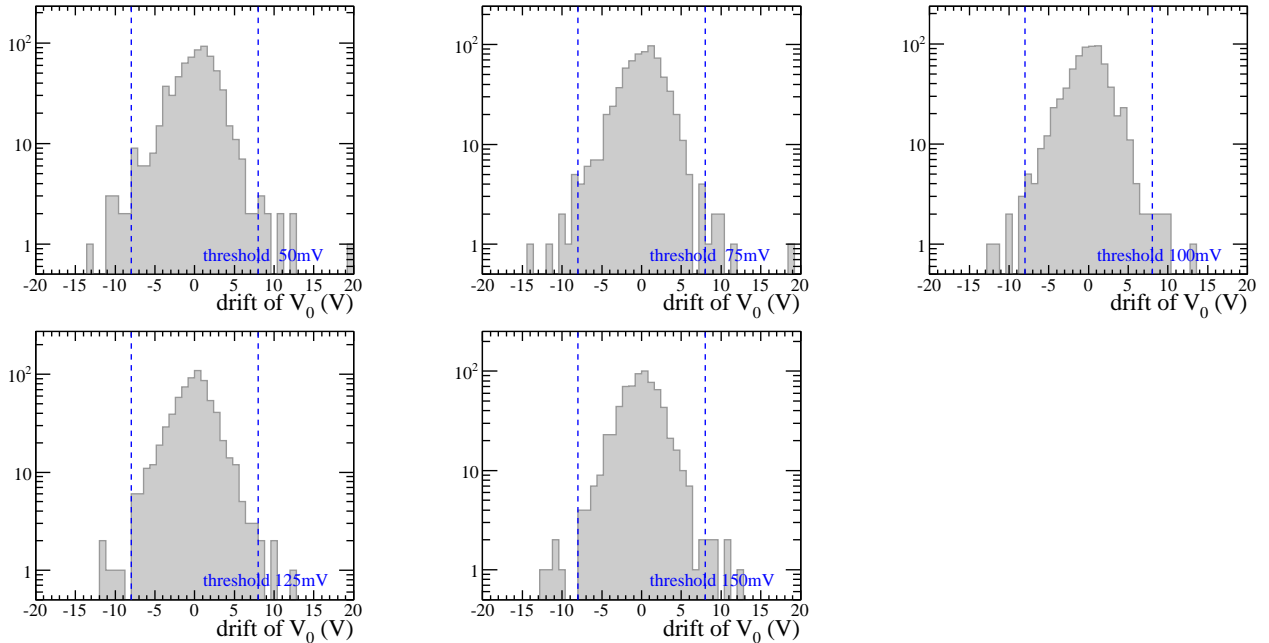


Figure 25: Drift of V_0 for each threshold measurement. Most of the retested PMTs had a drift value of less than ± 8 V, shown by the vertical dashed lines.

5.4 Final numbers

In summary, we have used three different criteria to select 2,900 PMTs out of the $\sim 3,100$ PMTs that are usable. The PMTs are divided into given a status of “good”, “retest”, “spare”, and “bad”. Table 3 shows how each criteria had an effect on the final selection.

The data from all of these measurements, as well as the status of each PMT, will be placed in a database created by FileMakerPro, and maintained by Dan Bennett during installation of the modules of the FCAL. Within the database, for each PMT we will have information on

- PMT ID (shown in barcode)
- run number with which data was taken
- channel used
- V_0 and λ for five separate threshold measurements

status		singly tested	retested	total
good		2436	—	2436
retest		—	463	463
spare	V_0 dist.	43	7	270
	aftercounts	16	182	
	drift of V_0	—	22	
bad		2	30	32

Table 3: Final numbers for the status of each PMT. The ones we will use in the final GlueX FCAL will be from the ones marked as “good” and “retest” (2899 total). There are approximately 270 PMTs marked as “spare”, which will be used if for some reason we run out of “good” and “retest”. The “bad” PMTs should not be used.

- fit coefficients A and B from fits to V_0 against threshold
- data of measurement
- status

For each retested PMT, there will be several entries for each PMT, which FileMakerPro will merge into one entry for that PMT. All of this information will be available as a database, and will help in diagnosing any problems seen in any particular module. The information will also be used to set the initial HV values for each PMT, so that we have gain balanced our modules to first order. After the beam is turned on and we have actual particles passing through, we will be able to further gain balance the detector with the use of the widths of π^0 and η particles.

5.5 Data files

If any further analysis of the PMT data is needed, all of the raw data is saved in ROOT format in `/s4/kmoriya/PMT/PMT-HV/dataFiles/` on the IU Task-D system. This data is also stored in the computer that took the data, mantrid01, and has a backup¹. All analysis source code and figures can also be found within `/s4/kmoriya/PMT/PMT-HV` within the IU Task-D system.

6 Conclusion

An overview of the tests done on the PMTs to be used for the GlueX FCAL have been presented. Most of the PMTs that were used in RadPhi and E852 are still usable, and show characteristics that are consistent with measurements that were done several years ago. The measured data will be placed in a database that will be accessible during GlueX running, and will allow us to diagnose each PMT individually. The criteria that was used to select the final PMTs was also given, and we have removed most of the PMTs that showed signs of an aging or bad PMT.

Acknowledgements

We would like to thank Paul Smith for technical support with the electronics and the setup in general, and also John Frye and Steve Martin for their many months of hard work in preparing and testing the PMTs.

¹contact Thom Sulanke, system administrator (tsulanke@indiana.edu) for details.